Published in final edited form as:
Anal Chem. 2013 July 16; 85(14): 6639–6645. doi:10.1021/ac4001332.

Assessing the Stochastic Intermittency of Single Quantum Dot Luminescence for Robust Quantification of Biomoleculs

Manuel. A. Palacios[1,2], **Michael M. Lacy**[1], **Stephanie M. Schubert**[1], **Mael Manesse**[1], and **David R. Walt**[1]

[1]Department of Chemistry, Tufts University, 62 Talbot Avenue, Medford, MA 02155

Abstract

Single molecule detection schemes promise the ability to reach the ultimate limit of detection: one molecule. In this paper, we use the stochastic luminescence of single semiconductor nanocrystals (Quantum dots, QDs) to detect and localize particles as digital counts. These digital counts can be correlated to the concentration of analytes in solution. Here, we use Total Internal Reflection Fluorescence (TIRF) microscopy to probe individual QDs immobilized on a functionalized substrate. QDs have found their niche in the bioanalytical community due to their remarkable brightness and stability. Despite their numerous outstanding photophysical properties, QDs at the single particle level display a pronounced intermittent luminescence, posing a challenge for the detection of individual particles. In this paper we demonstrate a reliable method for detecting QDs that takes advantage of these signal fluctuations by comparing the variations in the QD's fluorescence signals against variations of the background signal. The quantitative methodology developed here results in signal-to-background ratios up to 90:1, which is at least 8-times higher than the ratios obtained using methodologies relying solely on signal integration. This enhanced signal-to-background ratio facilitates a robust thresholding process and results infemtomolar limits of detection.

Introduction

This paper presents a methodology for digital quantification of biomolecules by detecting signal variations from single quantum dot (QD) reporters. QDs are highly fluorescent semiconductor nanocrystals that are widely used as labels for various biological and chemical applications.[1-5] Our method takes advantage of the stochastic blinking process intrinsic of QDs to measure the signal variation and compare it to variations of the background. Current detection techniques have achieved the ability to detect a single molecule;[6] however, in order to quantify single molecules, the development of methodologies that enable high efficiency detection of individual molecules is crucial. In this regard, signal processing techniques capable of precisely detecting most of the molecules within the probed area are of the utmost importance for future development of diagnostic tools with ultrasensitive LODs.

One of the most common problems associated with single molecule techniques based on digital quantification is the broad signal intensity distributions of the labels, which are due both to a lack of uniformity in the field of excitation and to the orientation of the molecular dipole moments.[7,8] In the case of single QD detection, there are two additional causes for signal distribution. First, the intrinsic polydispersity resulting from the fabrication process leads to different photophysical properties between different particles.[1] Second, single QDs

[2]Current address: GE Global Research, General Electric Company, 1 Research Circle, Niskayuna, NY 12309

possess a remarkable blinking behavior, where the luminescent state can be turned on and off stochastically for different periods of time.[9] As a result, even QDs with similar brightness at a given point in time can display very different signal-to-noise ratios when integrated over the entire observation time.

Digital quantification refers to the correlation between the number of 'quantifiable' molecules and the concentration of actual molecules within a solution.[7,8,10-15] The objective of this method is to be able to localize and count individual molecules. The main advantage of techniques that utilize digital quantification is a decrease in the probability of counting false positives. A disadvantage associated with most methods of digital quantification, however, is that the thresholding required to distinguish the widely distributed signals of individual QDs from the background often results in false negatives and ultimately in higher LODs.

In this paper, we present an alternative method for detecting signals from single QD reporters that produces higher signal-to-noise ratios. This is achieved by comparing the variation in single QD fluorescent signals over time to the variation in the background signal. There are several ways to assess variations or distribution of signals; our approach uses the standard deviation as a measure of the 'signal variations' over time. Using the standard deviation presents an advantage over traditional integration techniques because the background signal distribution decreases over time, while the resulting signal from intermittent reporters will be larger as they alternate between 'on' and 'off' states. Arguably, since the intermittent behavior is stochastic in nature, there could be QDs that remain in an 'on' state for the entire length of a measurement. Therefore, these signals will not yield a large standard deviation, but will have a large integrated signal. To account for this potential weakness, the method proposed here combines both the standard deviation and signal integration to acquire the final QD count. Our results demonstrate that by using this method, the number of single molecule counts can be increased by 25% compared to straight signal integration.

Experimental Section

PEG-SVA Functionalization on Amino-silanized Glass in PDMS Wells

The initial platform consisted of wells made out of a poly-dimethylsiloxane (PDMS) block that was fixed on a glass coverslip. Glass coverslips (No. 1.5 24 × 40mm, Fisher Scientific #12-544-C, glass thickness 0.16-0.19 mm) were cleaned and functionalized separately and the PDMS blocks with the well cut outs were fixed individually. All reagents were purchased from Sigma-Aldrich at molecular biology grade unless otherwise specified. CdSe/ZnS QDot 585 Streptavidin Conjugate was purchased from Invitrogen Corp (catalog number Q10111MP). PEG reagents were purchased from Laysan Bio, Inc.

Coverslips were cleaned by successive sonication in a glass staining dish for 20 minutes in a 10% Alconox suspension, 5 minutes in Milli-Q water, 10 minutes in acetone, 15 minutes in 1M KOH, and 10 minutes in Milli-Q water. Cleaned slides were stored in Milli-Q water until use. Prior to silanization the slides were dried under a continuous flow of dry nitrogen gas. Silanization with 3-aminopropyl-triethoxysilane (APTES) was carried out in a plastic staining dish with a mixture of 50 mL methanol, 2.5 mL acetic acid, and 0.5 mL APTES for 20 minutes, with sonication for one minute after the first ten minutes of reaction.

PDMS was prepared as a 10:1 mixture of PDMS base and elastomer, centrifuged at 1860×g for 2 minutes to remove bubbles, poured onto a flat petri dish, degassed under vacuum, and cured for 1 hour at 80°C. Holes for the wells were cut using a hole-punch, creating two 7 mm-diameter holes in the PDMS. The PDMS pieces were exposed to air plasma treatment

for 1 minute and immediately pressed onto cleaned, silanized, and dried coverslips to bond. A schematic of this assembly is shown in Figure 1. Wells produced in this way have a base surface area of 38.5 mm^2 and hold approximately 100 μL, though the well volume can vary as the thickness is determined when the PDMS layer is cast.

The surface of the glass was PEGylated using poly-(ethylene glycol) (PEG) modified with succinimidyl valerate ester (PEG-SVA). The reaction chemistry scheme is depicted in Figure1 below. The reaction mixture was prepared in a 40:1 ratio of methoxy-PEG-SVA and biotin-PEG-SVA, using 12.5 mg mPEG-SVA (MW 5000) and 0.31 mg biotin-PEG-SVA (MW 5000) per 100 μL of 0.1 M $NaHCO_3$ solution (pH 8.25) (concentrations 250 μM mPEG-SVA and 6.2 μM biotin-PEG-SVA). The solution was mixed thoroughly and centrifuged at 7200×g for 1 minute to remove bubbles. 40 μL of this mixture was added to each well and allowed to react overnight in a dark, humid chamber.

After this reaction, wells were washed with Milli-Q water. Surfaces were blocked by treating with 40 μL of BSA blocking solution (1% BSA in PBS) for 1 hour. This solution was removed and 40 μL of streptavidin-conjugated QD (SA-QD) solution (prepared at various dilutions in PBS with 1% BSA) was added to each well and allowed 15 minutes for surface binding. The SA-QD solution was removed and wells were washed three times with borate buffer (Thermo Scientific, contains 50 mM borate, pH 8.5) and then filled with borate buffer for imaging.

Samples were imaged using a Hamamatsu ImagEM EM-CCD camera on an Olympus IX-71 microscope configured for TIRF microscopy. The field of view with this configuration is 135 μm by 135 μm. Illumination source was a Melles Griot 561 nm diode-pumped solid-state laser, introduced through an Olympus APON 60×TIRF objective (1.49 NA). Images were recorded as 500 frame movies, at 32 frames/sec (approximately 15 sec total observation time) with sensitivity gain set at 180.

Image processing, analysis, and ImageJ macro code are provided in the Supporting Information.

Results and Discussions

In order to probe and study the signal of individual QDs, we first developed a simple assay that takes advantage of the strong biotin-streptavidin interaction (Figure 2). The strategy was to use streptavidin-quantum dots (SA-QDs) and immobilize them onto a biotin-functionalized glass surface to be probed by TIRF illumination. Briefly, the glass surface was modified with an amino-silane followed by addition of biotin-PEG-succinimidyl valerate (biotin-PEG-SVA), an amine-reactive ester forming a stable amide linkage on the surface. An important feature of this approach is that the PEG surface is known to reduce nonspecific protein adsorption.

Figure 3 shows typical signal traces of single SA-QD conjugates immobilized on a glass surface and illuminated by TIRF. A set of QDs will be intrinsically poly-disperse, and the non-uniformities in particle size, shape and composition can contribute to the differences observed in the signal. The examples here display different brightness maxima, blinking frequencies and off-times. Off-times range from many seconds to times shorter than the frame rate of the camera (~30 ms), a range spanning four orders of magnitude. Not only do different QDs display different behaviors, but also the same QD can exhibit different behaviors over time. An additional source of variation in the intensity is the physical location of the QD in the sample during TIRF illumination. Due to the exponential decay of the evanescent wave, small differences in the distance from the glass surface can cause significant changes in illumination intensity. Inconsistencies in the sample surface,

molecular motions, and different lengths of extension of the PEG surface molecules can all contribute to varying distances within the evanescent field. The bottom right panel of Figure 3 shows a box plot of the descriptive statistics of several single QD signals. It is worth noting that even though QD1 presents a higher signal maximum, its average signal is lower than the average signal measured for QD3, due mainly to an 'off' state for approximately 4 sec during the 15 seconds of signal collection. However, the standard deviation of the signal from QD1 is higher than QD3. In this study, we used commercially available QDs with a core/shell structure CdSe/ZnS that is known for its blinking behavior.[16,17] The blinking behavior of QDs is highly dependent on the nature and composition of the QDs used. For example, CdSe/CdS QDs with an intermediate shell thickness (7-9 monolayers) display a typical blinking behavior;[17] CdSe/CdS QDs bearing a thicker shell (16-19 monolayer) show nearly complete blinking suppression.[18]

Considering these behaviors in QD signal intensity, reliably detecting such an unpredictable signal can become a problem. The most obvious consideration is to expand the duration of the measurement. According to the inverse-power law, as the observation time increases, it becomes increasingly unlikely that a QD would have an off-time greater than the observation. Therefore, increasing the observation time increases the probability that fluorescence from any QD in the field of view will be captured by the camera. Nevertheless, due to the stochastic nature of the signal variation, longer collection time can still be a problem. Bentolila *et al.* warn that due to the power-law behavior of on- and off-times, increasing the integration time will not increase the time-integrated brightness linearly.[19] Therefore it is difficult to use this practice for reliable quantification of QDs. Crut *et al.* describe a detection method using a combination of the average and maximum values over a 60 sec measurement time, but still report that QD blinking can cause difficulty for reliable detection.[20]

An alternative way to detect and localize QDs is to probe the variations in the fluorescent signal. The standard deviation (the variance could also be used) is a measure of the variations or dispersion of a data set around its average, therefore the standard deviation could be used to characterize the signal of a QD compared to the background signal. Figure 4 (left) compares the progression, in time, of the signal-to-background ratios of the integrated signal and the standard deviation of the signal. In this experiment, two individual QDs were monitored simultaneously and both display similar emission intensity maxima during the 'on' state (~5410 photoelectrons). The plot shows that due to the high variations in the QD signal, compared to the small variations in the background signal, the standard deviation of the signal displayed a high contrast ratio between signal and background up to 90:1 for the traces in Figure 4, but it typically averages *ca.* 30:1. In comparison, signal integration resulted in contrast ratios *ca.* 13:1 in figure 4, but it averages *ca.* 4:1. Therefore, implementing the standard deviation for localization of QDs provides higher contrast ratios and consequently, more accurate and reliable detection compared to simple signal integration. It is worth noting that in theory, a signal fluctuating between two states (ON and OFF) stabilizes (plateaus) its standard deviation after approximately 10 switches.[21] In practice, the switching process between the ON and OFF states of the QDs is stochastic and could be longer than the experimental binning time. Also, the switching could commence prior to the binning time 'window' opens, or could end right before the binning time 'window' closes. The resulting photoluminescence intensities are not at the maximum (ON) or the minimum (OFF) states, but somewhere in between. Therefore, longer experiments have a higher probability of displaying a wider distribution of intensities and consequently higher signal-to-background ratios in the standard deviation 'channel'.

As a corollary, using higher excitation power could render a higher signal by increasing both intensity and variability because the blinking process would be more pronounced. Figure 4

(right) shows the correlation between the excitation power at the sample and the standard deviation of the fluorescent signal for the same QD over 60 s of data collection. Interestingly, there seems to be a quasi linear correlation between laser power and the standard deviation. Increasing the excitation power can potentially be used to enhance the signal-to-background ratio in the case of the standard deviation and also the integrated signal.

For the quantitative analysis of dilute analyte solutions, it is required that large areas of the capture surface are probed in order to ensure that there is a statistically significant number of molecules in the observation zone that exceed Poisson sampling noise. We used TIRFM imaging to study QD binding over an area of approximately 100×100 μm. We envisioned using a reasonably long observation time ~15s. For the analysis, image sequences were converted into a single image using various mathematical functions. This process called projecting, takes the intensity values of a pixel for each image in the sequence and applies a mathematical operation to these values. The resulting value is then used as the intensity of this pixel in a new projection image, as illustrated in Figure 5. We then use this image for further processing and analysis to count individual particles.

The method of stack integration is a useful way to capture the integration (or sum) and standard deviation of the signal from QD populations over time. Figure 6 shows two signal analysis histograms for the QD population. After comparing these different projection methods, the standard deviation projection provided the best signal-to-background ratio and the high contrast ratio allows the counting of QDs that otherwise would not be detected using simple integration. Both distributions have similar coefficients of variation (~0.6); thus, the improvement of the standard deviation method relies mostly on improvement in the signal-to-background ratio rather than the tightening of the signals distributions. Incorporating the standard deviation into our image analysis improves QD detection by about 10 to 15% compared to simply using the sum projection. This method addresses the different types of QD blinking behavior and improves detection using a relatively simple tool for image analysis.

Finally, some QDs could stay in the ‘on’ state for the duration of the observation. In such cases, the standard deviation would be relatively low, but the integrated signal would be high. In order to account for these cases, we incorporated both the sum and standard deviation projections. The sum and standard deviation projections are calculated and the two resulting images are normalized and merged into one composite image using the Merge Channels function (See Supporting Information for details). This process is illustrated in Figure 7.

Figure 8 shows the evolution of the digital counts against the number of images in a sequence collected over a period of time (up to ~15s). All methods plateau around 10s and, in the majority of the cases, the combined method gives higher numbers of QD counts in the time window.[22] As shown in Figure 8 (right), the complete analysis method, which uses a combination of the sum and standard deviation, averages 30% higher QD counts than the sum projection and 20% higher counts than the standard deviation projection alone. For benchmarking purposes, a ground truth level was established by counting QDs using visual inspection of the image sequences. The traces of each pixel were counted and compared to ensure that each positive count was derived from the presence of a single QD. The combination method accounts for *ca.* 95% of the ground truth level.[23] Furthermore, preliminary experiments showed that the combination method can be successfully implemented on data collected from epi-fluorescence setups, which present increased background noise.[24] When comparing data collected from the same field of view in TIRF and epi-fluorescence illumination modes, the final algorithm shows 6% (average) less

counts from the epi-fluorescence images. The latter attests to the robustness of this data analysis method and opens the door for the development of lower cost instrumentation for single molecule based assays.

To validate the quantification method, a calibration curve was established to correlate the digital counts on the probed surface to the concentration of SA-QDs in solution (Figure 9). The limit-of-detection (LOD) achieved is 5 fM and the dynamic range spans approximately 3 orders of magnitude. The LOD can be improved by probing larger areas, which can be achieved by scanning the surface. Alternatively, for the same amount of sample (~40 μl), if the biotin functionalized surface is confined to a smaller area than the total area probed, the molecules will be concentrated on the functionalized surface, and higher sensitivity can be achieved at the expense of incubation time and dynamic range. The upper limit of the dynamic range lowers due to digital saturation.[25] This approach can be achieved by combining our detection and analysis methods with a microfluidic platform. Using microfluidic channels, a tailored detection area can be defined and used to probe the entire sample. Preliminary experiments using microfluidic channels have shown a 4-fold increase in sensitivity using a *ca.* 400 times smaller sample size (~0.1 μl). Currently, further studies on this platform are underway.

Conclusions

In this paper we demonstrated the detection and localization of QDs using the standard deviation of the stochastic fluorescent signal traces. The method combines the signal integration over time with a calculation of the signal standard deviation to yield a robust method for quantifying single QDs. In the case of recently developed non-blinking or suppressed- blinking QDs,[18,26] our detection algorithm will at least perform as well as traditional integration methods.[27] Our method is rapid, automated and unbiased. It is able to account for *ca.* 95% of QDs in a field of view. The quantitative methodology developed here for digital quantification of single QDs enables detection at the femtomolar level, and should be suitable for bioanalytical applications such as quantification of low levels of DNA or protein targets. Further studies will focus on the development and integration of our methodology with a lab-on-a-chip system and with analytes of more biological interest.

Supplementary Material

Refer to Web version on PubMed Central for supplementary material.

Acknowledgments

We thank the Quanterix Corporation for providing financial support. We also thank Aaron Phillips for insightful discussions at the early stages of the project. Finally, we thank Mitchell Duffy for helping to improve the ImageJ code.

References

(1). Alivisatos AP. Science. 1996; 271:933.

(2). Bentolila, LA.; Michalet, X.; Weiss, S. Single Molecules and Nanotechnology. Rigler, R.; Vogel, H., editors. Springer-Verlag; Berlin Heidelberg: 2008. p. 53

(3). Bruchez M Jr. Moronne M, Gin P, Weiss S, Alivisatos AP. Science. 1998; 281:2013. [PubMed: 9748157]

(4). Chan WC, Nie S. Science. 1998; 281:2016. [PubMed: 9748158]

(5). Resch-genger U, Grabolle M, Cavaliere1jaricot S, Nitschke R, Nann T. Nature Methods. 2008; 5:763. [PubMed: 18756197]

(6). Walt DR. Analytical Chemistry. 2012

(7). Tessler, L. a.; Reifenberger, JG.; Mitra, RD. Analytical Chemistry. 2009; 81:7141. [PubMed: 19601620]

(8). Peterson EM, Harris JM. Analytical Chemistry. 2009; 82:189. [PubMed: 19957961]

(9). Nirmal M, Dabbousi BO, Bawendi MG, Macklin JJ, Trautman JK, Harris TD, Brus LE. Nature. 1996; 383:802.

(10). Cornish P, Ha T. ACS Chemical Biology. 2006; 2:53. [PubMed: 17243783]

(11). Fries JR, Brand L, Eggeling C, Köllner M, Seidel C. a. M. The Journal of Physical Chemistry A. 1998; 102:6601.

(12). Göransson J, Wählby C, Isaksson M, Howell WM, Jarvius J, Nilsson M. Nucleic Acids Research. 2009:37.

(13). Jarvius J, Melin J, Goransson J, Stenberg J, Fredriksson S, Gonzalez-Rey C, Bertilsson S, Nilsson M. Nature Methods. 2006; 3:725. [PubMed: 16929318]

(14). Rissin DM, Kan CW, Campbell TG, Howes SC, Fournier DR, Song L, Piech T, Patel PP, Chang L, Rivnak AJ, Ferrell EP, Randall JD, Provuncher GK, Walt DR, Duffy DC. Nature biotechnology. 2010; 28:595.

(15). Sui B, Li L, Li L, Jin W. The Analyst. 2011:6.

(16). Hamada M, Nakanishi S, Itoh T, Ishikawa M, Biju V. ACS Nano. 2010; 4:4445. [PubMed: 20731430]

(17). Galland C, Ghosh Y, Steinbruck A, Sykora M, Hollingsworth JA, Klimov VI, Htoon H. Nature. 2011; 479:203. [PubMed: 22071764]

(18). Chen Y, Vela J, Htoon H, Casson JL, Werder DJ, Bussian D. a. Klimov VI, Hollingsworth J. a. Journal of the American Chemical Society. 2008; 130:5026. [PubMed: 18355011]

(19). Bentolila, L. a.; Weiss, S. Cell biochemistry and biophysics. 2006; 45:59. [PubMed: 16679564]

(20). Crut A, Géron1Landre B, Bonnet I, Bonneau S, Desbiolles P, Escudé C. Nucleic acids research. 2005; 33:e98. [PubMed: 15967805]

(21). We are using the definition of the standard deviation for normally distributed data for our detection algorithm

(22). The influence of exposure time (frame rate) was studied and it is relatively small, compared to variations in digital counts, when different sections of the same sample are probed. Also, the increment in counts saturates at around 100ms. We chose a relatively short integration time (40 ms) to collect the data faster and to reduce the risk of sample drift that results in image smearing resulting in an inaccurate number of counts.

(23). The 5% (average) of particles not counted by the algorithm are very weak emitting QDs that have a similar standard deviation to the background and also are under threshold in the sum algorithm because of small differences in the illumination field

(24). See Supporting Information for experimental details and results

(25). Digital saturation refers to the limit at which the density of molecules on the probed surface is high enough that average distance between two particles is smaller than the difraction limit (optical resolution) of the system.

(26). Wang X, Ren X, Kahen K, Hahn M. a. Rajeswaran M, Maccagnano-Zacher S, Silcox J, Cragg GE, Efros AL, Krauss TD. Nature. 2009; 459:686. [PubMed: 19430463]

(27). Interestingly, in the case of non-blinking or suppressed-blinking QDs, the difference in the integrated signal intensity between single QDs will be given by the relative intensity of the QD under the experimental conditions of the observation. Therefore a narrower intensity distribution of the QD population can be expected due to suppression of the stochastic process. Preliminary observations on several QDs that stayed in the ON state for long periods of time show that even the variations in the ON state provided a boost in the signal-to-background ratio compared to integration methods.

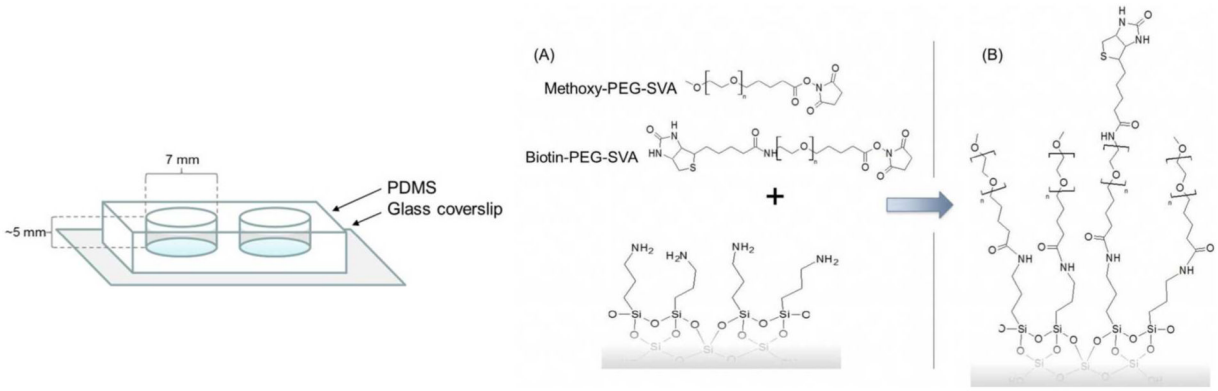

Figure 1. Left: PDMS wells on glass coverslip for PEG-biotin functionalization and SA-QD immobilization

Glass coverslips are cleaned and silanized before affixing PDMS wells. PEGylation and subsequent SA-QD binding is carried out in wells. **Right: Surface chemistry scheme.** PEG-SVA reagents react with amine groups on glass (A), producing amide linkages (B) with biotin groups scattered on the surface. For PEG MW 5000 g/mol, average length n = 114.

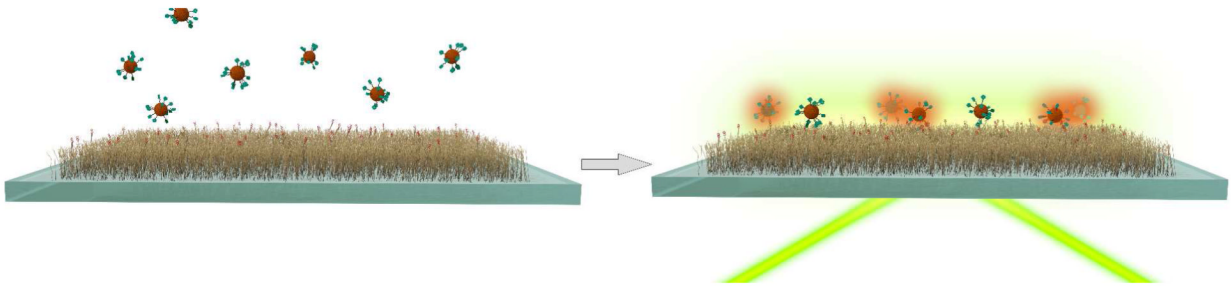

Figure 2.
QDs detection scheme. SA-QDs in solution bind to biotin on the PEG monolayer. TIRFM enables detection of QDs bound at the surface.

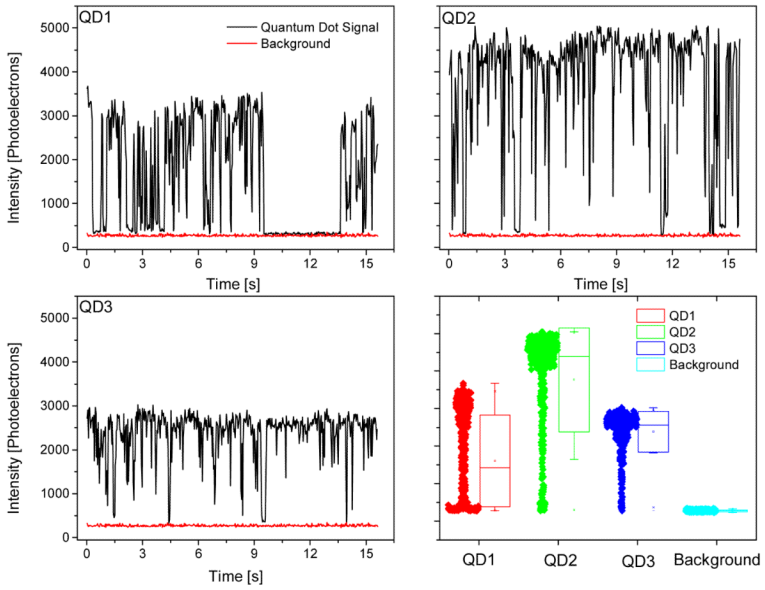

Figure 3.

Signal traces of three different single QDs monitored simultaneously. Bottom right: Raw data and boxplot displaying the descriptive statistics of the QD signals: the smallest observation (bottom whisker), standard deviation (box height), median (line in the box), mean (square centered in the box), and largest observation (upper whisker).

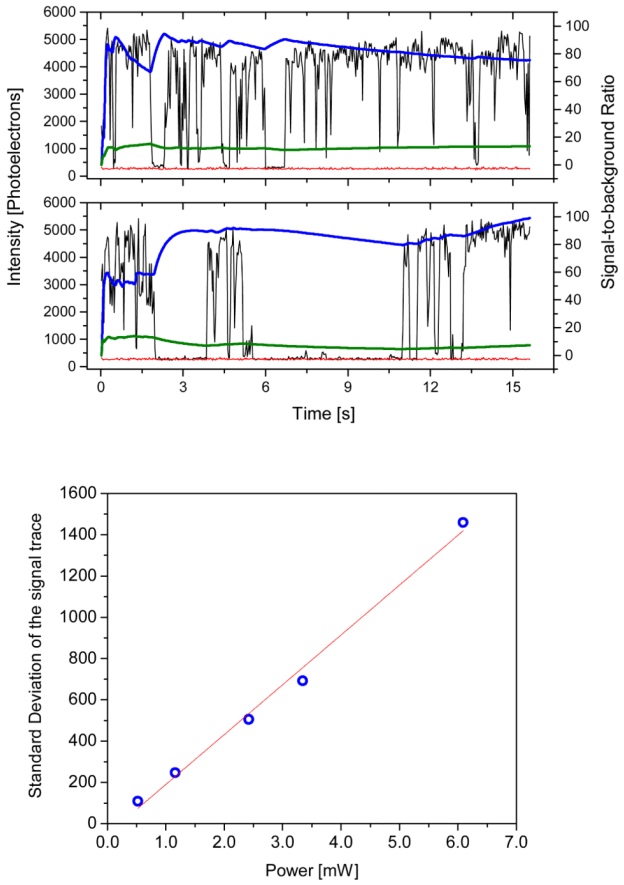

Figure 4.

Left: Signal traces of two different single QDs monitored simultaneously. (■■) QD signal, (■■) background signal, (■■) integrated signal-to-background ratio, and (■■) standard deviation of the signal to standard deviation of the background ratio. Right: Correlation between the laser power at the sample and the standard deviation of a single QD. The signal was recorded over 60 s.

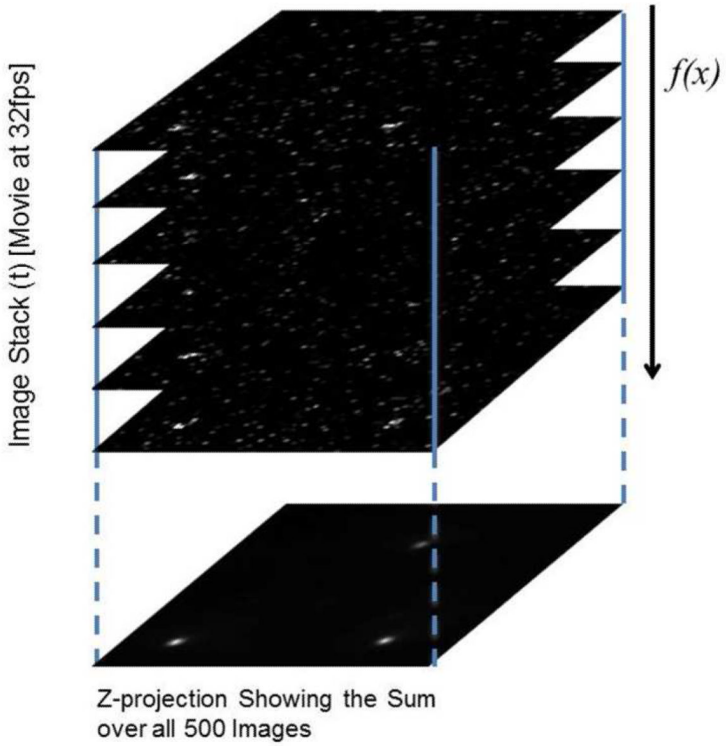

Figure 5.
Projection of an image stack. The movie is a 3-dimensional object, with each x and y in the image plane having a pixel intensity changing over time. Each pixel is treated as a function of time and a mathematical operation is applied, such as the sum.

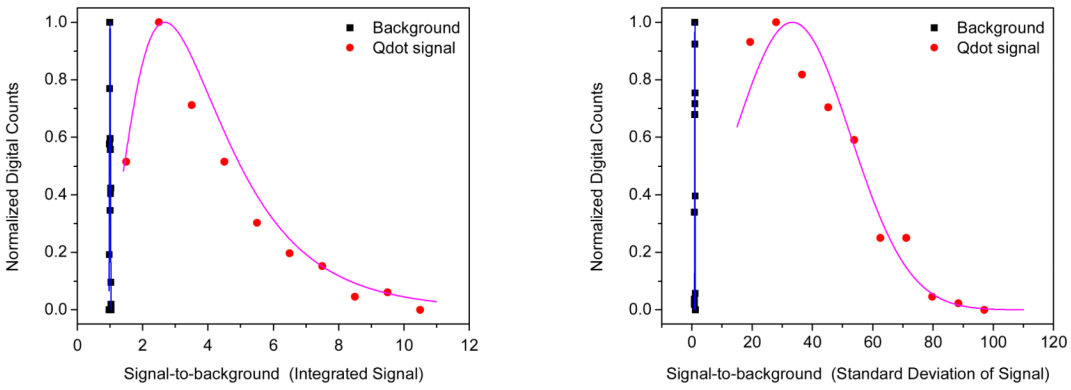

Figure 6.

Normalized histograms of the integrated signal signal-to-background ratios (left) fitted to a log normal distribution (left) the standard deviation of the signal fitted to a normal distribution (right). In both cases, the background signal fits a normal distribution.

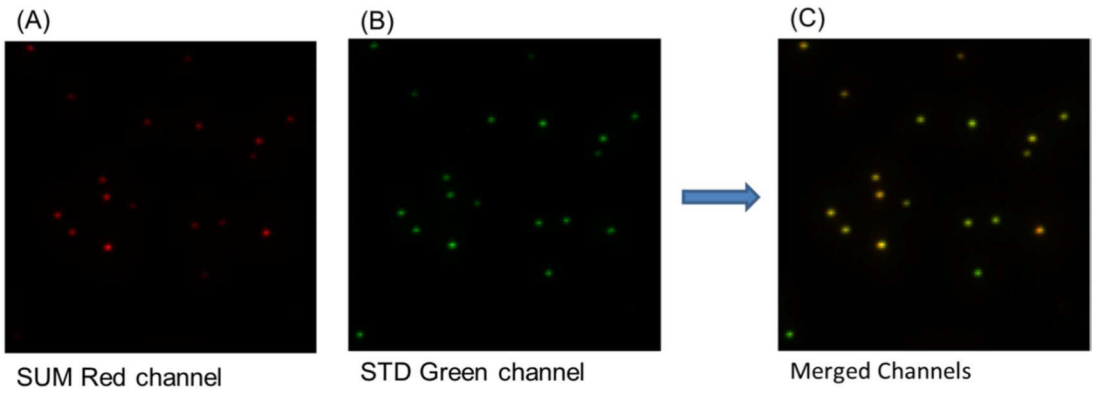

Figure 7. Merging SUM and STD projections

(A) and (B) are SUM and STD projections of the same sample image. Particles in the merged image (C) which appear more green were more intense in the STD projection, and vice versa. For example, the particle at the bottom left, which is hardly visible in the SUM projection, is detected due to its high signal in the STD projection. The image used in the figure represents only one region (1/16 = 6.5 × 6.5 μm) of the complete field of view.

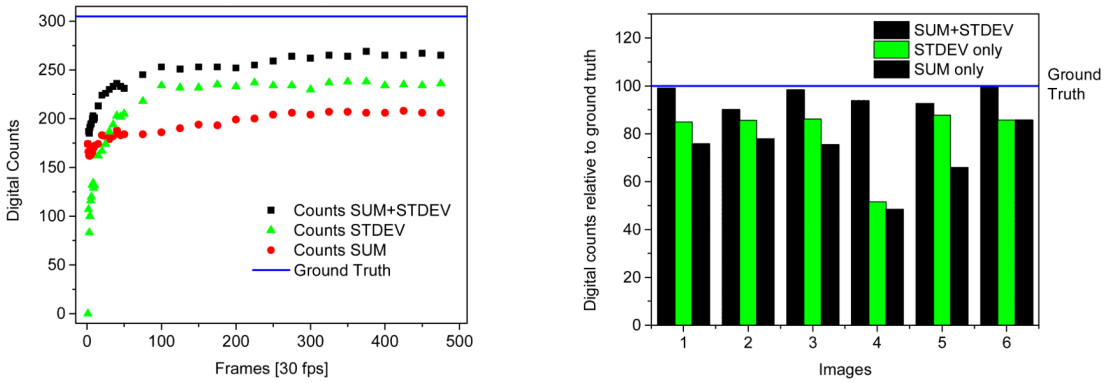

Figure 8.

Left: Digital counts as a function of frames (time). Right: Comparison of different projection methods for QD counting relative to the ground truth. The graph shows the results for 6 different images with varying concentrations of QDs. Red: QD counts using the sum projection. Green: QD counting using the standard deviation projection. Black: QD counts using the combination of the sum and the standard deviation projections. The actual numbers of counts are summarized in the Supporting Information.

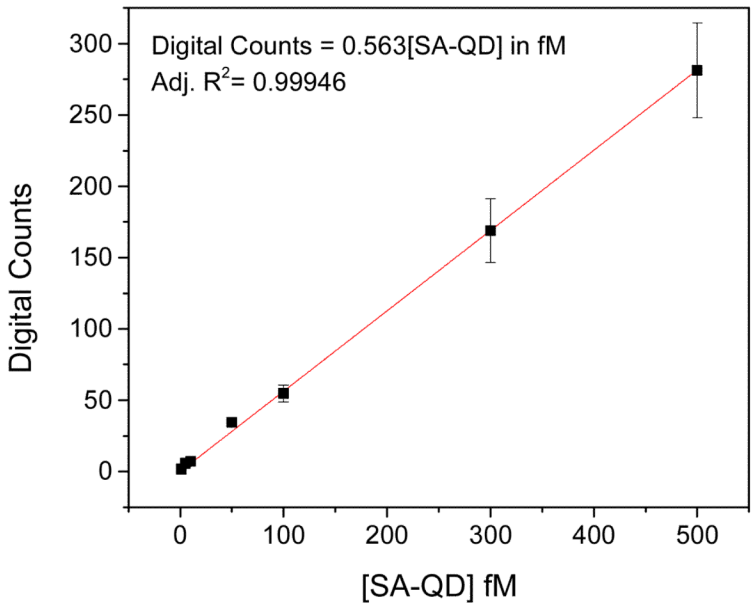

Figure 9.
Calibration curve correlating digital counts of SA-QD on the surface with the concentration of SA-QDs in solution.